

## A MARKER AND CELL TECHNIQUE FOR SOLVING TWO-DIMENSIONAL VISCOELASTIC FREE SURFACE FLOWS

**Murilo F. Tomé** – murilo@lcad.icmc.sc.usp.br

**Gerson F. Silva** – gersonfs@lcad.icmc.sc.usp.br

**Antonio Castelo Filho** – castelo@icmc.sc.usp.br

**José A. Cuminato** – jacumina@icmc.sc.usp.br

**Valdemir G. Ferreira** – valdemir@lcad.icmc.sc.usp.br

Universidade de São Paulo, Departamento de Ciências de Computação e Estatística

Cx.P. 668 – 13560-161 – São Carlos, SP, Brasil

**Sean McKee** – caas29@maths.strath.ac.uk

University of Strathclyde, Department of Mathematics

Glasgow, Scotland

### **Abstract.**

*This work presents the development of a numerical technique for simulating two-dimensional viscoelastic free surface flows of an Oldroyd-B fluid. The governing equations for an Oldroyd-B fluid are considered. The time derivative is approximated by a high order method. A novel formulation is developed for the computation of the non-Newtonian extra-stress components on rigid boundaries. The full free surface stress conditions are employed. The governing equations are solved by the finite difference method on a staggered grid. Numerical results demonstrating the capabilities of this numerical technique in solving two-dimensional flows of an Oldroyd-B fluid are given for a number of problems involving unsteady free surface flows. In addition, validation and convergence results are presented.*

**Keywords:** viscoelastic flow, Oldroyd-B, finite difference, constitutive equations.

### **1. Introduction**

The numerical simulation of fluid flow with free surfaces is important to many industrial applications. It is common, particularly in the processing industries, that the flow is unsteady, non-Newtonian, non-isothermal and possesses multiple free surfaces flowing in complex geometry. Moreover, in such industrial problems constitutive equations modelling such flows cannot be solved analytically so that only numerical solutions are invariably required. One of the main difficulties is how to formulate a technique which can impose the stress conditions on the free surface in such a way that the numerical solution approximates the physical solution accurately. Nonetheless, numerous researchers have attempted to solve this class of problems and a variety of methods have been presented, for instance, boundary integral techniques (Oguz & Prosperetti 1993), boundary element methods (eg. Phan-Thien et al. 1991), finite-element methods (eg. Marchal & Crochet 1987), Carew et al. 1993), Brasseur et al. 1998), methods using orthogonal coordinates (see Kang & Leal 1987, Asaithamb 1987) and Lagrangian methods (e.g. Fritts & Boris 1979). A different category of numerical techniques which have the potential for handling large surface deformations and surface folding and merging is that of volume tracking methods. These methods use a volumetric progress variable such as the cell volume fraction in the volume of fluid (VOF) technique (Hirt & Nichols 1981) for Lagrangian transport of the interfaces and the marker-and-cell (MAC) method (Harlow & Welch 1965) which employs marker-particles to represent the fluid interfaces. The MAC method has the advantage over the VOF method of easier logic programming which makes it attractive for developing computer codes to simulate free surface flows. It has been developed by various researchers (eg. Viacelli 1971, Chan & Street 1971, Amsden & Harlow 1970, Miyata & Nishimura 1985) and a detailed description of the technique can be found Tomé (1993). Recently, Castelo et al. (2001) developed the Freeflow3D code for simulating incompressible three-dimensional free surface flows. Freeflow3D is an extension of the GENSMAC code (Tomé & McKee 1994) to three dimensions. Like GENSMAC, Freeflow3D is a finite difference technique for solving incompressible flows using primitive variables on a staggered grid. However, many problems can be modelled by assuming two-dimensional flow and a two-dimensional version of Freeflow3D, denominated FreeFlow2D, has been developed. FreeFlow2D was constructed from FreeFlow3D by suppressing one of its coordinates. FreeFlow2D can cope with Newtonian free surface flows having complex shaped domains. Details of Freeflow2D can be found in (Oliveira & Castelo 1999). This work has the objective to extend the FreeFlow2D capabilities by incorporating a viscoelastic model within the framework of FreeFlow2D. We shall present a finite difference technique for solving the Oldroyd-B model and incorporate it into the FreeFlow2D code. This paper is organized as follows: Section 2 gives the governing equations of an incompressible Oldroyd-B fluid flow and Section 3 describes a numerical method for solving the basic equations. Section 4 presents the finite difference discretization; Section 5 gives validation results and presents some numerical results.

## 2. Governing Equations

The basic equations governing the incompressible flow of an Oldroyd-B fluid are the equations of motion and the mass conservation equation together with the constitutive equation for the Oldroyd-B model, which can be written as (see Tomé et al. 2002):

$$\rho \frac{Dv_i}{Dt} = -\frac{\partial p}{\partial x_i} + \mu_0 \left( \frac{\lambda_2}{\lambda_1} \right) \frac{\partial}{\partial x_k} \left( \frac{\partial v_i}{\partial x_k} + \frac{\partial v_k}{\partial x_i} \right) + \frac{\partial S_{ik}}{\partial x_k} + \rho g_i, \quad \frac{\partial v_i}{\partial x_i} = 0, \quad (1)$$

$$S_{ik} + \lambda_1 \overset{\nabla}{S}_{ik} = 2\mu_0 \left( 1 - \frac{\lambda_2}{\lambda_1} \right) d_{ik}, \quad (2)$$

where  $S_{ik}$  is the non-Newtonian symmetric extra-stress tensor. The upper convected derivative  $\overset{\nabla}{S}_{ik}$  is defined by

$$\overset{\nabla}{T}_{ik} = \frac{\partial T_{ik}}{\partial t} + v_m \frac{\partial T_{ik}}{\partial x_m} - \frac{\partial v_i}{\partial x_m} T_{mk} - \frac{\partial v_k}{\partial x_m} T_{im} \quad \text{and} \quad d_{ik} = \frac{1}{2} \left( \frac{\partial v_i}{\partial x_k} + \frac{\partial v_k}{\partial x_i} \right)$$

is the rate-of-deformation tensor and  $\lambda_1$  and  $\lambda_2$  are time constants (relaxation and retardation) and  $\mu_0$  is the solution viscosity. The vector  $v_i$ , ( $i = 1, 2$ ) denotes the velocity,  $p$  the pressure,  $\rho$  the density and  $g_i$ , ( $i = 1, 2$ ) the components of gravity.  $\frac{D}{Dt}$  denotes the material derivative. We observe that by making  $\lambda_2 = 0$  we obtain the Maxwell model.

We consider two-dimensional flows and by letting  $L, U$  and  $\nu_0$  denote ‘‘typical’’ length, velocity and viscosity scales, we introduce the nondimensionalization

$$u = U\bar{u}, \quad v = U\bar{v}, \quad x = L\bar{x}, \quad z = L\bar{z}, \quad t = \frac{L}{U}\bar{t}, \quad p = \rho U^2 \bar{p}, \quad \nu = \nu_0 \bar{\nu}, \quad S_{i,k} = \rho U^2 \tilde{S}_{i,k}, \quad \mathbf{g} = g\bar{\mathbf{g}},$$

which upon introduction into Eqs. (1)–(2) produces the following nondimensional equations (the bars have been dropped for convenience)

$$\frac{\partial u}{\partial t} + \frac{\partial u^2}{\partial x} + \frac{\partial(uv)}{\partial y} = -\frac{\partial p}{\partial x} + \frac{1}{Re} \left( \frac{\lambda_2}{\lambda_1} \right) \left( \frac{\partial^2 u}{\partial x^2} + \frac{\partial^2 u}{\partial y^2} \right) + \left( \frac{\partial S^{xx}}{\partial x} + \frac{\partial S^{xy}}{\partial y} \right) + \frac{1}{Fr^2} g_x \quad (3)$$

$$\frac{\partial v}{\partial t} + \frac{\partial(uv)}{\partial x} + \frac{\partial v^2}{\partial y} = -\frac{\partial p}{\partial y} + \frac{1}{Re} \left( \frac{\lambda_2}{\lambda_1} \right) \left( \frac{\partial^2 v}{\partial x^2} + \frac{\partial^2 v}{\partial y^2} \right) + \left( \frac{\partial S^{xy}}{\partial x} + \frac{\partial S^{yy}}{\partial y} \right) + \frac{1}{Fr^2} g_y \quad (4)$$

$$\frac{\partial u}{\partial x} + \frac{\partial v}{\partial y} = 0 \quad (5)$$

$$S^{xx} + We \left( \frac{\partial S^{xx}}{\partial t} + \frac{\partial u S^{xx}}{\partial x} + \frac{\partial v S^{xx}}{\partial y} - 2 \frac{\partial u}{\partial x} S^{xx} - 2 \frac{\partial u}{\partial y} S^{xy} \right) = \frac{2}{Re} \left( 1 - \frac{\lambda_2}{\lambda_1} \right) \frac{\partial u}{\partial x} \quad (6)$$

$$S^{yy} + We \left( \frac{\partial S^{yy}}{\partial t} + \frac{\partial u S^{yy}}{\partial x} + \frac{\partial v S^{yy}}{\partial y} - 2 \frac{\partial v}{\partial x} S^{xy} - 2 \frac{\partial v}{\partial y} S^{yy} \right) = \frac{2}{Re} \left( 1 - \frac{\lambda_2}{\lambda_1} \right) \frac{\partial v}{\partial y} \quad (7)$$

$$S^{xy} + We \left( \frac{\partial S^{xy}}{\partial t} + \frac{\partial u S^{xy}}{\partial x} + \frac{\partial v S^{xy}}{\partial y} - \frac{\partial v}{\partial x} S^{xx} - \frac{\partial u}{\partial y} S^{yy} \right) = \frac{1}{Re} \left( 1 - \frac{\lambda_2}{\lambda_1} \right) \left( \frac{\partial u}{\partial y} + \frac{\partial v}{\partial x} \right) \quad (8)$$

respectively, where  $Re = \nu_0/UL$  denotes the Reynolds number,  $We = \lambda_1(U/L)$  is the Weissenberg number,  $Fr = U/\sqrt{Lg}$  is the Froude number.  $L, U$  and  $\nu_0$  denote ‘‘typical’’ length, velocity and viscosity scales, respectively.

## 3. Boundary Conditions

In order to solve Eqs. (4)–(9) one needs to impose boundary conditions for  $\mathbf{u}$  and  $\mathbf{S}$ . For the momentum equations we assume the no-slip condition  $\mathbf{u} = \mathbf{0}$  on solid boundaries is valid.

### 3.1 Computation of the stress on rigid boundaries

Equations (6)–(8) will be solved by a high order upwinding scheme which requires the values of the non-Newtonian extra stress  $\mathbf{S}$  on rigid boundaries. As rigid boundaries may be regarded as characteristics, the stresses  $S^{xx}$ ,  $S^{yy}$  and  $S^{xy}$  on the boundary are computed from Eqs. (4)–(6), which we assume to hold on rigid boundaries with the initial condition  $\mathbf{S} = \mathbf{0}$ . We introduce the change of variables  $\mathbf{S} = e^{-\frac{t}{We}} \tilde{\mathbf{S}}$  into Eqs. (4)–(6) obtaining the equations

$$\left( \frac{\partial \tilde{S}^{xx}}{\partial t} + u \frac{\partial \tilde{S}^{xx}}{\partial x} + v \frac{\partial \tilde{S}^{xx}}{\partial y} - 2 \frac{\partial u}{\partial x} \tilde{S}^{xx} - 2 \frac{\partial u}{\partial y} \tilde{S}^{xy} \right) = \frac{1}{We} \frac{2}{Re} \left( 1 - \frac{\lambda_2}{\lambda_1} \right) e^{\frac{1}{We}t} \frac{\partial u}{\partial x} \quad (9)$$

$$\left( \frac{\partial \tilde{S}^{yy}}{\partial t} + u \frac{\partial \tilde{S}^{yy}}{\partial x} + v \frac{\partial \tilde{S}^{yy}}{\partial y} - 2 \frac{\partial v}{\partial x} \tilde{S}^{xy} - 2 \frac{\partial v}{\partial y} \tilde{S}^{yy} \right) = \frac{1}{We} \frac{2}{Re} \left( 1 - \frac{\lambda_2}{\lambda_1} \right) e^{\frac{1}{We}t} \frac{\partial v}{\partial y} \quad (10)$$

$$\left( \frac{\partial \tilde{S}^{xy}}{\partial t} + u \frac{\partial \tilde{S}^{xy}}{\partial x} + v \frac{\partial \tilde{S}^{xy}}{\partial y} - \frac{\partial v}{\partial x} \tilde{S}^{xx} - \frac{\partial u}{\partial y} \tilde{S}^{yy} \right) = \frac{1}{We} \frac{1}{Re} \left( 1 - \frac{\lambda_2}{\lambda_1} \right) e^{\frac{1}{We}t} \left( \frac{\partial u}{\partial y} + \frac{\partial v}{\partial x} \right) \quad (11)$$

Now, making use of the no-slip condition equations Eqs. (9)-(11) can be easily solved for the stress components  $S^{xx}$ ,  $S^{yy}$  and  $S^{xy}$ . If we consider solid boundaries parallel to the  $x$ -axis, it can be shown that the components of the non-Newtonian extra stress are given by (for details see Tomé et al. 2002)

$$S^{xx}(x, y, t + \delta t) = e^{-\frac{1}{We}\delta t} S^{xx}(x, y, t) + \delta t \left[ \frac{\partial u}{\partial y}(x, y, t) e^{-\frac{1}{We}\delta t} \frac{\partial}{\partial x} S^{xy}(x, y, t) + \frac{\partial u}{\partial y}(x, y, t + \delta t) S^{xy}(x, y, t + \delta t) \right], \quad (12)$$

$$S^{yy}(x, y, t) = 0, \quad S^{xy}(x, y, t + \delta t) = e^{-\frac{1}{We}\delta t} S^{xy}(x, y, t) + \frac{1}{Re} \left( 1 - \frac{\lambda_2}{\lambda_1} \right) \frac{\partial u}{\partial y}(x, y, t^*) \left[ 1 - e^{-\frac{1}{We}\delta t} \right]. \quad (13)$$

It can be shown that the components of the non-Newtonian extra stress tensor on solid boundaries which are parallel to the  $y$ -axis are given by

$$S^{xx}(x, y, t) = 0, \quad S^{xy}(x, y, t + \delta t) = e^{-\frac{1}{We}\delta t} S^{xy}(x, y, t) + \frac{1}{Re} \left( 1 - \frac{\lambda_2}{\lambda_1} \right) \frac{\partial v}{\partial x}(x, y, t^*) \left[ 1 - e^{-\frac{1}{We}\delta t} \right], \quad (14)$$

$$S^{yy}(x, y, t + \delta t) = e^{-\frac{1}{We}\delta t} S^{yy}(x, y, t) + \delta t \left[ \frac{\partial v}{\partial x}(x, y, t) e^{-\frac{1}{We}\delta t} S^{xy}(x, y, t) + \frac{\partial v}{\partial x}(x, y, t + \delta t) S^{xy}(x, y, t + \delta t) \right] \quad (15)$$

### 3.2 Inflow and Outflow boundaries

These can be specified as follows:

- **Inflow boundary:** At the fluid entrance we can impose the velocity components  $u_n = U$  and  $u_\tau = 0$  while for the non-Newtonian extra stress tensor components  $\mathbf{S}$  we adopt the strategy of Mompean & Deville (1999), namely:  $S^{xx} = 0$ ,  $S^{xy} = 0$  and  $S^{yy} = 0$ .
- **Outflow boundary:** At fluid exit we impose homogeneous Neumann conditions for both the velocity components and the extra stress components, namely  $\frac{\partial u_n}{\partial n} = \frac{\partial u_\tau}{\partial n} = 0$  and  $\frac{\partial S^{xx}}{\partial n} = \frac{\partial S^{xy}}{\partial n} = \frac{\partial S^{yy}}{\partial n} = 0$ . In the equations above the subscripts  $n$  and  $\tau$  denote directions normal and tangential to the boundary, respectively.

### 3.3 Free Surface Stress Conditions

At the free surface the normal and tangential stresses must be zero (see Batchelor 1967). If we consider two-dimensional cartesian flows than the stress conditions can be written as

$$p - \frac{2}{Re} \frac{\lambda_2}{\lambda_1} \left[ \frac{\partial u}{\partial x} n_x^2 + \left( \frac{\partial u}{\partial y} + \frac{\partial v}{\partial x} \right) n_x n_y + \frac{\partial v}{\partial y} n_y^2 \right] + S^{xx} n_x^2 + 2S^{xy} n_x n_y + S^{yy} n_y^2 = 0, \quad (16)$$

$$\frac{1}{Re} \frac{\lambda_2}{\lambda_1} \left[ 2 \left( \frac{\partial v}{\partial y} - \frac{\partial u}{\partial x} \right) n_x n_y + \left( \frac{\partial u}{\partial y} + \frac{\partial v}{\partial x} \right) (n_x^2 - n_y^2) \right] + (S^{yy} - S^{xx}) n_x n_y + S^{xy} (n_x^2 - n_y^2) = 0. \quad (17)$$

## 4. Method of Solution

To solve Eqs. (3)-(8) we employ the procedure presented by (Tomé et al. 2002). We suppose that for a given time, say  $t_n$ , the velocity field  $\mathbf{u}(\mathbf{x}, t_n)$  and the non-Newtonian extra stress tensor  $\mathbf{S}(\mathbf{x}, t_n)$  are known and the pressure field  $\tilde{p}(\mathbf{x}, t_n)$  satisfies the pressure condition on the free surface. We compute the velocity field, pressure field and the non-Newtonian extra-stress tensor at the advanced time  $t_{n+1} = t_n + \delta t$ , in the following steps:

i : Calculate the intermediate velocity field,  $\tilde{\mathbf{u}}(\mathbf{x}, t_{n+1})$ , from

$$\frac{\partial \tilde{u}}{\partial t} = -\frac{\partial(u^2)}{\partial x} - \frac{\partial(uv)}{\partial y} - \frac{\partial \tilde{p}}{\partial x} + \frac{1}{Re} \left( \frac{\lambda_2}{\lambda_1} \right) \left( \frac{\partial^2 u}{\partial x^2} + \frac{\partial^2 u}{\partial y^2} \right) + \left( \frac{\partial S^{xx}}{\partial x} + \frac{\partial S^{xy}}{\partial y} \right) + \frac{1}{Fr^2} g_x \quad (18)$$

$$\frac{\partial \tilde{v}}{\partial t} = -\frac{\partial(uv)}{\partial x} - \frac{\partial v^2}{\partial y} - \frac{\partial \tilde{p}}{\partial y} + \frac{1}{Re} \left( \frac{\lambda_2}{\lambda_1} \right) \left( \frac{\partial^2 v}{\partial x^2} + \frac{\partial^2 v}{\partial y^2} \right) + \left( \frac{\partial S^{xy}}{\partial x} + \frac{\partial S^{yy}}{\partial y} \right) + \frac{1}{Fr^2} g_y \quad (19)$$

with  $\tilde{\mathbf{u}}(\mathbf{x}, t_n) = \mathbf{u}(\mathbf{x}, t_n)$  using the correct boundary conditions for  $\mathbf{u}(\mathbf{x}, t_n)$ . These equations are solved by the finite difference method.

ii : Solve the Poisson equation:  $\nabla^2 \psi(\mathbf{x}, t_{n+1}) = \nabla \cdot \tilde{\mathbf{u}}(\mathbf{x}, t_{n+1})$ . The appropriate boundary conditions for this equation are:  $\frac{\partial \psi}{\partial n} = 0$  on solid boundaries and  $\psi = 0$  on the free surface.

iii : Compute the velocity field:  $\mathbf{u}(\mathbf{x}, t_{n+1}) = \tilde{\mathbf{u}}(\mathbf{x}, t_{n+1}) - \nabla \psi(\mathbf{x}, t_{n+1})$ .

iv : Compute the pressure:  $p(\mathbf{x}, t_{n+1}) = \tilde{p}(\mathbf{x}, t_n) + \frac{\psi(\mathbf{x}, t_{n+1})}{\delta t}$ .

v : Update the components of the non-Newtonian extra-stress tensor on rigid boundaries according to the equations given in Section 3.1

vi : Compute the components of the non-Newtonian extra-stress tensor,  $S^{xx}(\mathbf{x}, t_{n+1})$ ,  $S^{xy}(\mathbf{x}, t_{n+1})$ ,  $S^{yy}(\mathbf{x}, t_{n+1})$ , from:

$$\frac{\partial S^{xx}}{\partial t} = \left[ -\frac{\partial(uS^{xx})}{\partial x} - \frac{\partial(vS^{xx})}{\partial y} + 2\frac{\partial u}{\partial x}S^{xx} + 2\frac{\partial v}{\partial y}S^{xy} + \frac{1}{We} \frac{1}{Re} \left[ 2 \left(1 - \frac{\lambda_2}{\lambda_1}\right) \frac{\partial u}{\partial x} - S^{xx} \right] \right]_{t_n}, \quad (20)$$

$$\frac{\partial S^{yy}}{\partial t} = \left[ -\frac{\partial(uS^{yy})}{\partial x} - \frac{\partial(vS^{yy})}{\partial y} + 2\frac{\partial v}{\partial x}S^{xy} + 2\frac{\partial u}{\partial y}S^{yy} + \frac{1}{We} \frac{1}{Re} \left[ 2 \left(1 - \frac{\lambda_2}{\lambda_1}\right) \frac{\partial v}{\partial y} - S^{yy} \right] \right]_{t_n}, \quad (21)$$

$$\frac{\partial S^{xy}}{\partial t} = \left[ -\frac{\partial(uS^{xy})}{\partial x} - \frac{\partial(vS^{xy})}{\partial y} + \frac{\partial v}{\partial x}S^{xx} + \frac{\partial u}{\partial y}S^{yy} + \frac{1}{We} \frac{1}{Re} \left[ \left(1 - \frac{\lambda_2}{\lambda_1}\right) \left( \frac{\partial u}{\partial y} + \frac{\partial v}{\partial x} \right) - S^{xy} \right] \right]_{t_n}. \quad (22)$$

Equations (20)–(22) are solved by finite differences. Details of the difference equations are given in the next Section.

vii : Update the markers positions: The last step in the calculation is to move the markers to their new positions. This is done by solving

$$\frac{dx}{dt} = u, \quad \frac{dy}{dt} = v, \quad (23)$$

for each particle. The fluid surface is defined by a list containing these markers and the visualization of the free surface is obtained simply by connecting them by straight lines.

## 5. Finite Difference Approximation

To implement the algorithm presented in Section 4 (see eqs. (18)-(22)) we employ the finite difference method as follows. A staggered grid is employed and typical cell is displayed in figure 1a. The components of the non-Newtonian extra-stress tensor together with the pressure field are applied at the centre of a cell while the velocity components  $u$  and  $v$  are staggered by  $\delta x/2$  and  $\delta y/2$ , respectively. As the fluid is continuously moving, a scheme to identify the fluid region and the fluid free surface is employed. To accommodate this, the cells within the mesh are flagged as boundary cells (B), empty cells (E), full cells (F), surface cells (S), inflow cells (I) and outflow cells (O). A detailed description of these types of cells can be found in Tomé et al. (Tomé et al. 2002). Figure 1b illustrates the types of cells used by Freeflow2D.

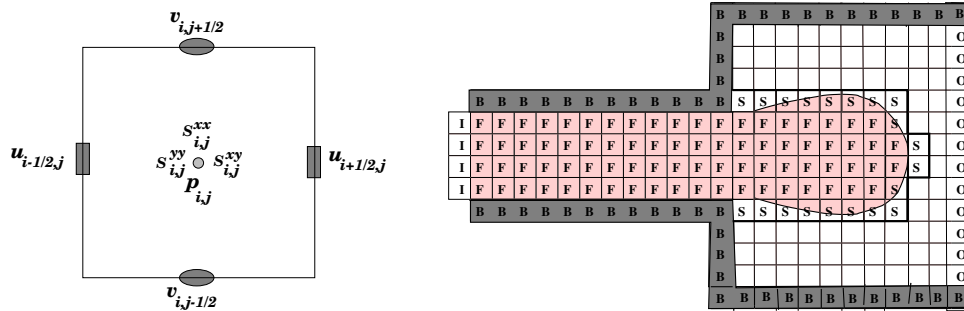


Figure 1. Typical cell for an Oldroyd-B fluid flow calculation.

When solving the tilde equations (18)-(19), it is usual to approximate the time derivative explicitly by the well known Euler method which is of first order (see Tomé et al. 2002). In this work we shall approximate the time derivative by the explicit modified Euler method which is second order in time. The pressure gradient is approximated by central differences and the laplacian operator is discretized using second order differences. The convective terms are approximated by the VONOS scheme which is a high order upwind method. Details of the VONOS scheme can be found in (Ferreira et al. 2002). The terms involving the components of the non-Newtonian extra-stress tensor inn (18) are approximated by central differences,

$$\frac{\partial S^{xx}}{\partial x} \Big|_{i+\frac{1}{2},j} = \frac{S^{xx}_{i+1,j} - S^{xx}_{i,j}}{\delta x}, \quad \frac{\partial S^{xy}}{\partial y} \Big|_{i+\frac{1}{2},j} = \frac{S^{xy}_{i+\frac{1}{2},j+\frac{1}{2}} - S^{xy}_{i+\frac{1}{2},j-\frac{1}{2}}}{\delta y}, \quad (24)$$

where terms like  $S^{xy}_{i+\frac{1}{2},j+\frac{1}{2}}$  are obtained by averaging the four nearest values, e.g.  $S^{xy}_{i+\frac{1}{2},j+\frac{1}{2}} := (S^{xy}_{i,j} + S^{xy}_{i+1,j} + S^{xy}_{i,j+1} + S^{xy}_{i+1,j+1})/4$ . However, if the cell  $(i, j)$  is adjacent to a B-cell (Tomé et al. 2002) use a forward difference or a backward difference to approximate  $\frac{\partial S^{xy}}{\partial y} \Big|_{i+\frac{1}{2},j}$ . In this work we make use of a Taylor series expansion for the cell  $(i, j)$  and approximate the derivative  $\frac{\partial S^{xy}}{\partial y} \Big|_{i+\frac{1}{2},j}$  by a second order scheme. For instance, if the cell  $(i, j)$  has a B-cell above it we use the approximation  $\frac{\partial S^{xy}}{\partial y} \Big|_{i+\frac{1}{2},j} = \frac{S^{xy}_{i+\frac{1}{2},j} + 3S^{xy}_{i+\frac{1}{2},j-1} - 4S^{xy}_b}{\delta y}$  while if the B-cell is below the cell  $(i, j)$  then it is approximated by  $\frac{\partial S^{xy}}{\partial y} \Big|_{i+\frac{1}{2},j} = -\frac{S^{xy}_{i+\frac{1}{2},j} + 3S^{xy}_{i+\frac{1}{2},j-1} - 4S^{xy}_b}{\delta y}$ . The same procedure is applied to the derivative  $\frac{\partial S^{xy}}{\partial x} \Big|_{i,j+\frac{1}{2}}$

appearing in the  $v$ -tilde calculation (19). If the cell  $(i, j)$  is a surface cell (S) the treatment for approximating the derivatives  $\frac{\partial S^{xy}}{\partial y} \Big|_{i+\frac{1}{2},j}$  and  $\frac{\partial S^{xy}}{\partial x} \Big|_{i,j+\frac{1}{2}}$  is the same as for cells which are adjacent to  $B$ -cells. Thus, Eqs. (18) and (19) are approximated by

$$\begin{aligned} u_{i+\frac{1}{2},j}^* &= u_{i+\frac{1}{2},j} + \delta t F(u, v), & v_{i,j+\frac{1}{2}}^* &= v_{i,j+\frac{1}{2}} + \delta t G(u, v) \\ \tilde{u}_{i+\frac{1}{2},j} &= u_{i+\frac{1}{2},j} + \frac{\delta t}{2} [F(u^*, v^*) + F(u, v)], & \tilde{v}_{i,j+\frac{1}{2}} &= v_{i,j+\frac{1}{2}} + \frac{\delta t}{2} [G(u^*, v^*) + G(u, v)] \end{aligned} \quad (25)$$

where

$$\begin{aligned} F(u, v) &= \left[ -\mathbf{conv}(u^2) - \mathbf{conv}(uv) - \frac{\tilde{p}_{i+1,j} - \tilde{p}_{i,j}}{\delta x} + \left( \frac{\partial S^{xx}}{\partial x} \Big|_{i+\frac{1}{2},j} + \frac{\partial S^{xy}}{\partial y} \Big|_{i+\frac{1}{2},j} \right) \right. \\ &\quad \left. + \frac{1}{Re} \left( \frac{\lambda_2}{\lambda_1} \right) \left( \frac{u_{i-\frac{1}{2},j} - 2u_{i+\frac{1}{2},j} + u_{i+\frac{3}{2},j}}{\delta x^2} + \frac{u_{i+\frac{1}{2},j-1} - 2u_{i+\frac{1}{2},j} + u_{i+\frac{1}{2},j+1}}{\delta y^2} \right) + \frac{1}{Fr^2} g_x \right], \\ G(u, v) &= \left[ -\mathbf{conv}(vu) - \mathbf{conv}(v^2) - \frac{\tilde{p}_{i,j+1} - \tilde{p}_{i,j}}{\delta y} + \left( \frac{\partial S^{xy}}{\partial x} \Big|_{i,j+\frac{1}{2}} + \frac{\partial S^{yy}}{\partial y} \Big|_{i,j+\frac{1}{2}} \right) - \frac{1}{Fr^2} g_y \right. \\ &\quad \left. + \frac{1}{Re} \left( \frac{\lambda_2}{\lambda_1} \right) \left( \frac{v_{i-1,j+\frac{1}{2}} - 2v_{i,j+\frac{1}{2}} + v_{i+1,j+\frac{1}{2}}}{\delta x^2} + \frac{v_{i,j-\frac{1}{2}} - 2v_{i,j+\frac{1}{2}} + v_{i,j+\frac{3}{2}}}{\delta y^2} \right) \right]. \end{aligned}$$

We would like to point out that the approximations described for discretizing the momentum equations are second order accurate in time and space. In a similar manner, the components of the non-Newtonian extra stress Eqs. (20)-(22) are approximated by finite differences. The time derivative is explicitly approximated by the modified Euler method, the convective terms are computed using the VONOS method and the spatial first order derivatives are second order accurate. Thus,  $S^{xx}$ ,  $S^{xy}$  and  $S^{yy}$  are computed as follows:

$$S_{i,j}^{xx*} = S_{i,j}^{xx} + H_1(S^{xx}, S^{xy}, S^{yy}), \quad S_{i,j}^{xy*} = S_{i,j}^{xy} + H_2(S^{xx}, S^{xy}, S^{yy}), \quad S_{i,j}^{yy*} = S_{i,j}^{yy} + H_3(S^{xx}, S^{xy}, S^{yy}),$$

$$S_{i,j}^{xx(n+1)} = S_{i,j}^{xx} + \frac{\delta t}{2} [H_1(S^{xx}, S^{xy}, S^{yy}) + H_1(S^{xx*}, S^{xy*}, S^{yy*})],$$

$$S_{i,j}^{xy(n+1)} = S_{i,j}^{xy} + \frac{\delta t}{2} [H_2(S^{xx}, S^{xy}, S^{yy}) + H_2(S^{xx*}, S^{xy*}, S^{yy*})],$$

$$S_{i,j}^{yy(n+1)} = S_{i,j}^{yy} + \frac{\delta t}{2} [H_3(S^{xx}, S^{xy}, S^{yy}) + H_3(S^{xx*}, S^{xy*}, S^{yy*})]$$

where

$$\begin{aligned} H_1(S^{xx}, S^{xy}, S^{yy}) &= -\left( \frac{1}{We} \right) S_{i,j}^{xx} - \left[ \mathbf{conv}(uS^{xx})_{i,j} + \mathbf{conv}(vS^{xx})_{i,j} - 2 \frac{(u_{i+\frac{1}{2},j} - u_{i-\frac{1}{2},j})}{\delta x} S_{i,j}^{xx} \right. \\ &\quad \left. - 2 \frac{(u_{i,j+\frac{1}{2}} - u_{i,j-\frac{1}{2}})}{\delta y} S_{i,j}^{xy} + \frac{2}{We} \left( \frac{\lambda_2}{\lambda_1} - 1 \right) \frac{(u_{i+\frac{1}{2},j} - u_{i-\frac{1}{2},j})}{\delta x} \right], \end{aligned} \quad (26)$$

$$\begin{aligned} H_2(S^{xx}, S^{xy}, S^{yy}) &= -\left( \frac{1}{We} \right) S_{i,j}^{xy} - \left[ \mathbf{conv}(uS^{xy})_{i,j} + \mathbf{conv}(vS^{xy})_{i,j} - \frac{(v_{i+\frac{1}{2},j} - v_{i-\frac{1}{2},j})}{\delta x} S_{i,j}^{xx} \right. \\ &\quad \left. - \frac{(u_{i,j+\frac{1}{2}} - u_{i,j-\frac{1}{2}})}{\delta y} S_{i,j}^{yy} + \frac{1}{We} \left( \frac{\lambda_2}{\lambda_1} - 1 \right) \left( \frac{u_{i,j+\frac{1}{2}} - u_{i,j-\frac{1}{2}}}{\delta y} + \frac{v_{i+\frac{1}{2},j} - v_{i-\frac{1}{2},j}}{\delta x} \right) \right], \end{aligned} \quad (27)$$

$$\begin{aligned} H_3(S^{xx}, S^{xy}, S^{yy}) &= -\left( \frac{1}{We} \right) S_{i,j}^{yy} - \left[ \mathbf{conv}(uS^{yy})_{i,j} + \mathbf{conv}(vS^{yy})_{i,j} - 2 \frac{(v_{i,j+\frac{1}{2}} - v_{i,j-\frac{1}{2}})}{\delta y} S_{i,j}^{yy} \right. \\ &\quad \left. - 2 \frac{(v_{i+\frac{1}{2},j} - v_{i-\frac{1}{2},j})}{\delta x} S_{i,j}^{xy} + \frac{2}{We} \left( \frac{\lambda_2}{\lambda_1} - 1 \right) \frac{(v_{i,j+\frac{1}{2}} - v_{i,j-\frac{1}{2}})}{\delta y} \right]. \end{aligned} \quad (28)$$

In equations (26)–(28), terms which are not defined at cell position are obtained by averaging, that is:

$$u_{i,j+\frac{1}{2}} := \frac{u_{i+\frac{1}{2},j} + u_{i+\frac{1}{2},j+1} + u_{i-\frac{1}{2},j} + u_{i-\frac{1}{2},j+1}}{4}, \quad v_{i+\frac{1}{2},j} := \frac{v_{i,j+\frac{1}{2}} + v_{i+1,j+\frac{1}{2}} + v_{i,j-\frac{1}{2}} + v_{i+1,j-\frac{1}{2}}}{4}. \quad (29)$$

The Poisson equation (see step iv Section 3) is discretized at cell centres using the five-point Laplacian, namely,

$$\frac{\psi_{i+1,j} - 2\psi_{i,j} + \psi_{i-1,j}}{\delta x^2} + \frac{\psi_{i,j+1} - 2\psi_{i,j} + \psi_{i,j-1}}{\delta y^2} = \frac{\tilde{u}_{i+\frac{1}{2},j} - \tilde{u}_{i-\frac{1}{2},j}}{\delta x} + \frac{\tilde{v}_{i,j+\frac{1}{2}} - \tilde{v}_{i,j-\frac{1}{2}}}{\delta y}. \quad (30)$$

Equation (30) leads to a symmetric and positive definite linear system for  $\psi_{i,j}$ . In order to solve this linear system we employ the conjugate gradient method as implemented in GENSMAC (see Tomé et al. 1996). The final velocities are obtained by (see step iii, Section 3):

$$u_{i+\frac{1}{2},j}^{n+1} = \tilde{u}_{i+\frac{1}{2},j} - \left( \frac{\psi_{i+1,j} - \psi_{i,j}}{\delta x} \right), \quad v_{i,j+\frac{1}{2}}^{n+1} = \tilde{v}_{i,j+\frac{1}{2}} - \left( \frac{\psi_{i,j+1} - \psi_{i,j}}{\delta y} \right). \quad (31)$$

The pressure is obtained by (see step iv, Section 3):  $p_{i,j} = \tilde{p}_{i,j} + \frac{\psi_{i,j}}{\delta t}$ .

## 5.1 Free Surface Stress Conditions

On the free surface, Eqs. (16) and (17) are expected to hold. They are imposed on every surface cell by considering the local orientation of the free surface. For instance, if a surface cell has only one face in contact with an empty cell than the free surface is considered to either horizontal or vertical. In this case, we take  $\mathbf{n} = (1, 0)$  or  $\mathbf{n} = (0, 1)$  so that equations (16) and (17) simplify to

$$\tilde{p} - \frac{2}{Re} \frac{\lambda_2}{\lambda_1} \frac{\partial u_n}{\partial n} + S^{nn} = 0 \quad \text{and} \quad \frac{2}{Re} \frac{\lambda_2}{\lambda_1} \left( \frac{\partial u}{\partial y} + \frac{\partial v}{\partial x} \right) + S^{xy} = 0, \quad \text{where } n \text{ is either } x \text{ or } y. \quad (32)$$

Equation (32) and the mass equation Eq. (5) are employed to compute the pressure  $\tilde{p}_{i,j}$  and the velocities at the free surface. These are computed using the same methodology given by (Tomé et al 2002). On the other hand, if a surface cell has only two adjacent faces which are in contact with empty cell faces than the free surface is considered to be at  $45^\circ$  with the coordinate axes. For these cells we take  $\mathbf{n} = \left( \pm \frac{\sqrt{2}}{2}, \pm \frac{\sqrt{2}}{2} \right)$ . In this case Eqs. (16) and (17) reduce to

$$\tilde{p} - \text{sign}(n_x n_y) \frac{1}{Re} \frac{\lambda_2}{\lambda_1} \left( \frac{\partial u}{\partial y} + \frac{\partial v}{\partial x} \right) + S^{xx} + S^{yy} + 2 \text{sign}(n_x n_y) S^{xy} = 0, \quad \text{sign}(n_x n_y) \left[ \frac{2}{Re} \frac{\lambda_2}{\lambda_1} \left( \frac{\partial v}{\partial y} - \frac{\partial u}{\partial x} \right) + S^{yy} - S^{xx} \right] = 0. \quad (33)$$

Equation (33) and the mass equation Eq. (5) are used to calculate the pressure and the velocities on surface cells which have two adjacent faces in contact with empty cell faces. Details of finite difference involved can be found in (Tomé et al 2002).

## 5.2 Computation of the non-Newtonian extra-stress components on solid surfaces

When the discretized momentum equations and the discretized non-Newtonian extra stress equations are applied at nodes that are adjacent to the boundary then the values of  $S^{xx}$ ,  $S^{yy}$  and  $S^{xy}$  on the boundary cells are required.

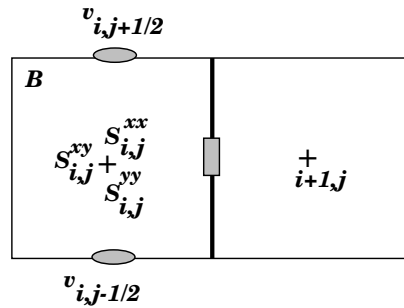


**Fig. 2.** B-cell having only the  $(i + \frac{1}{2})$  face in contact with an interior cell.

They can be obtained by using the equations derived in Section 3.1 and by inspecting the boundary cells. For instance, if a B-cell has only the  $(i + \frac{1}{2})$ -face in contact with an interior cell we assume that the solid boundary is parallel to the  $y$ -axis. In this case, Eqs. (14) and (15) give

$$S^{xx}_{i+\frac{1}{2},j} = 0, \quad S^{xy}_{i+\frac{1}{2},j}(t_{n+1}) = e^{-\frac{1}{We} \delta t} S^{xy}(t_n) + \left(1 - \frac{\lambda_2}{\lambda_1}\right) \frac{\partial v}{\partial x}(x_{i+\frac{1}{2}}, y_j, t^*) \left[ e^{\frac{1}{We} \delta t} - 1 \right] \quad (34)$$

$$S^{yy}_{i+\frac{1}{2},j}(t_{n+1}) = e^{-\frac{1}{We} \delta t} S^{yy}(t_n) + \delta t \frac{\partial v}{\partial x}(x_{i+\frac{1}{2}}, y_j, t^*) \left[ e^{-\frac{1}{We} \delta t} S^{xy}(t_n) + S^{xy}(t_{n+1}) \right] \quad (35)$$

where  $\frac{\partial v}{\partial x}(x_{i+\frac{1}{2}}, y_j, t^*)$  is obtained by averaging  $\frac{\partial v}{\partial x}(x_{i+\frac{1}{2}}, y_j, t)$  at times  $t_n$  and  $t_{n+1}$ , namely

$$\frac{\partial v}{\partial x}(x_{i+\frac{1}{2}}, y_j, t^*) = \frac{1}{2} \left[ \frac{\partial v}{\partial x}(x_{i+\frac{1}{2}}, y_j, t_n) + \frac{\partial v}{\partial x}(x_{i+\frac{1}{2}}, y_j, t_{n+1}) \right].$$

These derivatives are approximated by expanding  $v$  in a Taylor series at the point  $(x_{i+\frac{1}{2}}, y_j, t_n)$  as follows:

$$v(x, y_j, t_n) = v(x_{i+\frac{1}{2}}, y_j, t_n) + h \frac{\partial v}{\partial x}(x_{i+\frac{1}{2}}, y_j, t_n) + \frac{h^2}{2!} \frac{\partial^2 v}{\partial x^2}(x_{i+\frac{1}{2}}, y_j, t_n) + \frac{h^3}{3!} \frac{\partial^3 v}{\partial x^3}(\xi_i, y_j, t_n) \quad (36)$$

where  $h = (x - x_{i+\frac{1}{2}})$ . Evaluating (36) at  $x = x_{i+1}$  and  $x = x_{i+2}$  we obtain

$$v(x_{i+1}, y_j, t_n) = v(x_{i+\frac{1}{2}}, y_j, t_n) + \frac{\delta x}{2} \frac{\partial v}{\partial x}(x_{i+\frac{1}{2}}, y_j, t_n) + \frac{\delta x^2}{8} \frac{\partial^2 v}{\partial x^2}(x_{i+\frac{1}{2}}, y_j, t_n) + \frac{\delta x^3}{48} \frac{\partial^3 v}{\partial x^3}(\xi_i, y_j, t_n), \quad (37)$$

$$v(x_{i+2}, y_j, t_n) = v(x_{i+\frac{1}{2}}, y_j, t_n) + \frac{3\delta x}{2} \frac{\partial v}{\partial x}(x_{i+\frac{1}{2}}, y_j, t_n) + \frac{9\delta x^2}{8} \frac{\partial^2 v}{\partial x^2}(x_{i+\frac{1}{2}}, y_j, t_n) + \frac{27\delta x^3}{48} \frac{\partial^3 v}{\partial x^3}(\xi_i, y_j, t_n). \quad (38)$$

Multiplying (37) by -9 and adding to (38) and solving for  $\frac{\partial v}{\partial x}(x_{i+\frac{1}{2}}, y_j, t_n)$  we obtain the second order approximation (since  $v(x_{i+\frac{1}{2}}, y_j, t_n) = 0$  due to the no-slip condition)

$$\frac{\partial v}{\partial x}(x_{i+\frac{1}{2}}, y_j, t_n) = \frac{3v_{i+1,j} - v_{i+2,j}/3}{\delta x}, \quad v_{i,j} = \frac{v_{i,j+\frac{1}{2}} + v_{i,j-\frac{1}{2}}}{2}, \quad v_{i+1,j} = \frac{v_{i+1,j+\frac{1}{2}} + v_{i+1,j-\frac{1}{2}}}{2}. \quad (39)$$

The required values of  $S_{i,j}^{xx}$  and  $S_{i,j}^{yy}$  are then computed by linear interpolation using the nodes  $(i + \frac{1}{2}, j)$  and  $(i + 1, j)$ . Boundary cells having the left side contiguous with an interior cell are treated similarly. On the other hand, if a B-cell has only the top face in contact with one interior cell then we assume the solid boundary is parallel to the  $x$ -axis in which case Eqs. (12) and (13) give

$$S^{xx}(x_i, y_{j+\frac{1}{2}}, t_{n+1}) = e^{-\frac{1}{We}\delta t} S^{xx}(x_i, y_{j+\frac{1}{2}}, t_n) + \delta t \left[ \frac{\partial u}{\partial y}(x_i, y_{j+\frac{1}{2}}, t_n) e^{-\frac{1}{We}\delta t} S^{xy}(x_i, y_{j+\frac{1}{2}}, t_n) + \frac{\partial u}{\partial y}(x_i, y_{j+\frac{1}{2}}, t_{n+1}) S^{xy}(x_i, y_{j+\frac{1}{2}}, t_{n+1}) \right], \quad (40)$$

$$S^{yy}(x_i, y_{j+\frac{1}{2}}, t_{n+1}) = 0, \quad S^{xy}(x_i, y_{j+\frac{1}{2}}, t_{n+1}) = e^{-\frac{1}{We}\delta t} S^{xy}(x_i, y_{j+\frac{1}{2}}, t_n) + \frac{1}{Re} \left(1 - \frac{\lambda_2}{\lambda_1}\right) \frac{\partial u}{\partial y}(x_i, y_{j+\frac{1}{2}}, t_n) \left[1 - e^{-\frac{1}{We}\delta t}\right]. \quad (41)$$

The derivative  $\frac{\partial u}{\partial y}(x_i, y_{j+\frac{1}{2}}, t_n)$  is evaluated in the same manner as  $\frac{\partial u}{\partial x}(x_{i+\frac{1}{2}}, y_j, t_n)$ . We take the Taylor series at  $(x_i, y_{j+\frac{1}{2}}, t_n)$  and apply it at the points  $(x_i, y_{j+1}, t_n)$  and  $(x_i, y_{j+2}, t_n)$  and solving for  $\frac{\partial u}{\partial y}(x_i, y_{j+\frac{1}{2}}, t_n)$  we obtain the second order approximation

$$\frac{\partial u}{\partial y}(x_i, y_{j+\frac{1}{2}}, t_n) = \frac{u_{i,j+1} - u_{i,j+2}/3}{\delta y}, \quad u_{i,j+1} = \frac{u_{i+\frac{1}{2},j+1} + u_{i-\frac{1}{2},j+1}}{2}, \quad u_{i,j+2} = \frac{u_{i+\frac{1}{2},j+2} + u_{i-\frac{1}{2},j+2}}{2}. \quad (42)$$

## 6. Validation and numerical results

The finite difference equations presented in this work have been implemented into the FREEFLOW2D code (see Castelo et al. 1999) in order to simulate free surface flow of an Oldroyd-B fluid.

### 6.1 Fully developed channel flow

We validate the numerical treatment for calculating the viscoelastic extra-stress tensor on rigid boundaries and on interior points by simulating the flow in a two-dimensional channel. We consider a 2D-channel formed by two parallel walls at a distance  $L$  from each other and having a length of  $5L$  (see Fig. 3). At the channel entrance we impose the analytical profiles of fully developed flow and at the exit the conditions presented in this paper for outflow boundaries are employed. On the channel walls the no-slip condition and the expressions for the viscoelastic extra-stress tensor (see Section 3.1) are applied. We start with the channel empty and inject fluid at the inflow at a prescribed velocity. The fully developed flow imposed at the inflow is given by

$$u(y) = -4\frac{U}{L}(y - L/2)^2 + U, \quad v = 0 \quad (43)$$

$$S^{xx}(y) = 2We \frac{1}{Re} \left(1 - \frac{\lambda_2}{\lambda_1}\right) \left(\frac{\partial u}{\partial y}\right)^2, \quad S^{xy} = \frac{1}{Re} \left(1 - \frac{\lambda_2}{\lambda_1}\right) \left(\frac{\partial u}{\partial y}\right), \quad S^{yy} = 0 \quad (44)$$

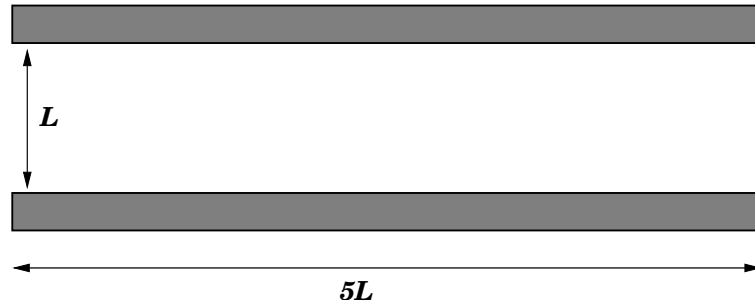
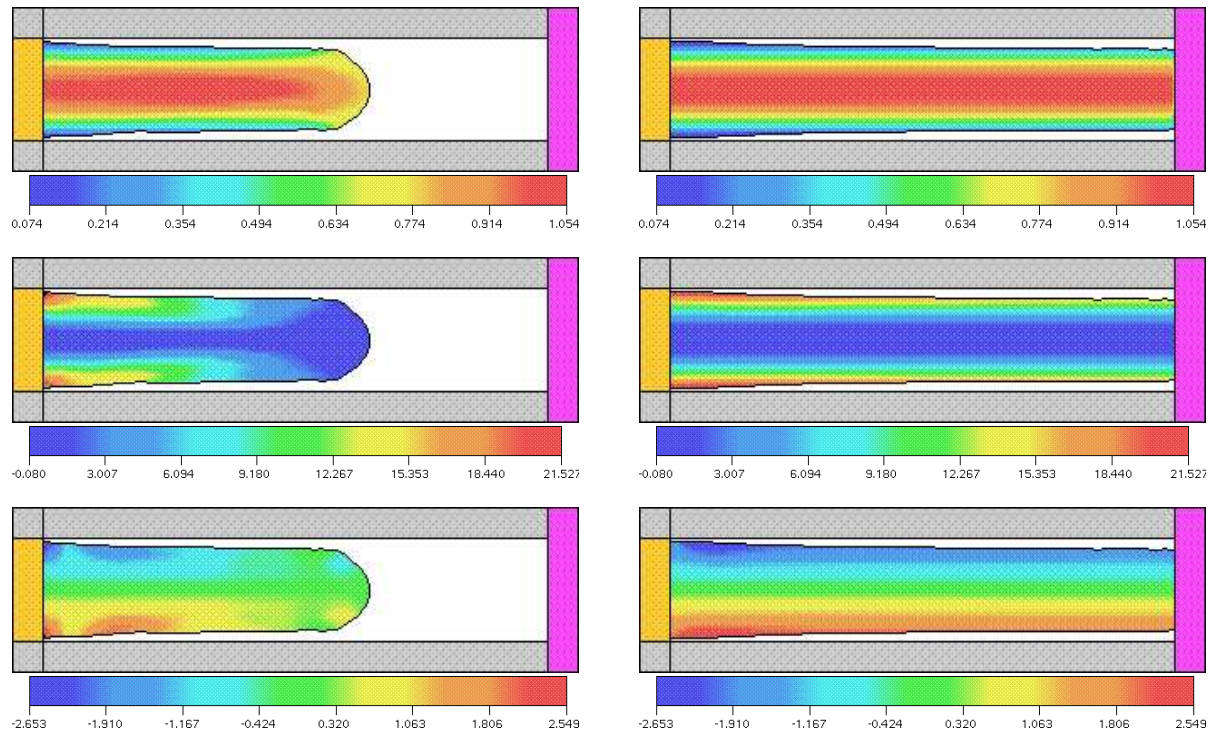


Figure 3. Channel flow set up parameters.

To simulate this problem we used the following input data  $L = 1$ ,  $U = 1$ ,  $\nu = 1$ ,  $\lambda_1 = 2$  and the ratio  $\lambda_2/\lambda_1$  was set equal to 0.5. Hence  $Re = LU/\nu = 1$  and  $We = \lambda_1 U/L = 2$ . To verify the convergence of the numerical method proposed in this work we run this problem on three meshes as follows: Mesh1 -  $\delta x = \delta y = 0.2$  ( $5 \times 25$  cells); Mesh2 -  $\delta x = \delta y = 0.1$  ( $10 \times 50$  cells) and Mesh3 -  $\delta x = \delta y = 0.05$  ( $20 \times 100$  cells). Initially the channel is empty and fluid is injected at the inflow until it reaches the outflow and steady state is established. Under steady state conditions the velocity field and the viscoelastic extra-stress on the channel must have the same values as those on the inflow. Figure 4 displays snapshots taken from the simulation on Mesh2 at different times. Figure 5 displays the calculated values of the velocity  $u$  and the values of the non-Newtonian extra-stress component  $S^{xx}$  at the line  $x = 2.5$  (middle of the channel) together with the respective analytic values (see Eqs. (43)(44)) on Mesh1, Mesh2 and Mesh3, respectively. As we can see in Fig. 5 the agreement between the exact and the numerical solutions is very good. Indeed, the relative  $l_2$ -norm of the errors,

$$E^{xy} = \frac{\sum (S_{exact}^{xy} - S_{numerical}^{xy})^2}{\sum (S_{exact}^{xy})^2}, \quad E^{xx} = \frac{\sum (S_{exact}^{xx} - S_{numerical}^{xx})^2}{\sum (S_{exact}^{xx})^2}$$

are  $E^{xy} = 0.001138$ ,  $E^{xx} = 0.005839$  on Mesh1,  $E^{xy} = 0.000579$  and  $E^{xx} = 0.002201$  on Mesh2 and  $E^{xy} = 0.00038$ ,  $E^{xx} = 0.00179$  on Mesh3. These results demonstrate the convergence of the numerical method presented in this paper.



**Figure 4.** Numerical simulation of the channel flow. Fluid surface and velocity contours of the  $u$ -velocity and the components of the non-Newtonian extra stress  $S^{xx}$  and  $S^{xy}$ , respectively. Times shown are  $t = 4$  (on the left) and  $t = 100$  (on the right).

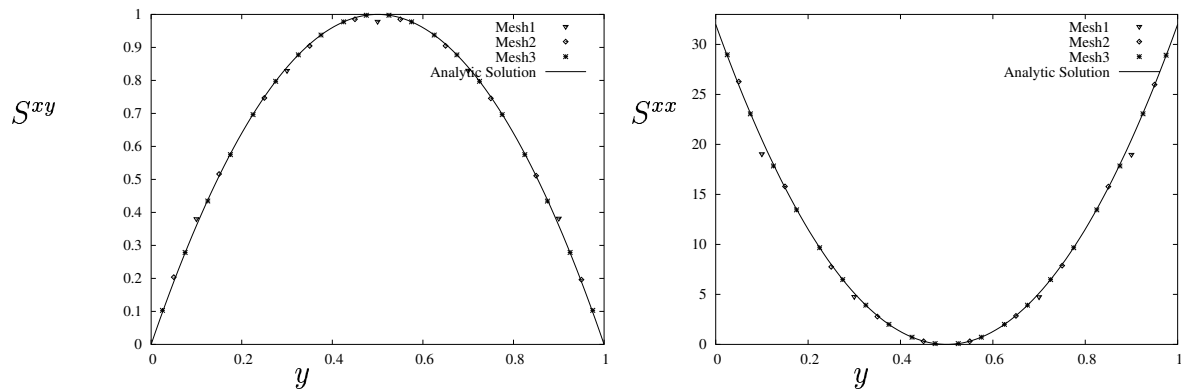


**Figure 5.** Numerical and analytic solutions of the velocity  $u$  and the component of the non-Newtonian stress  $S^{xx}$  at time  $t = 50$  at position  $x = 2.5$ .

## 6.2 Numerical simulation of the transient extrudate swell of a planar jet

To demonstrate that the numerical method presented in this paper can simulate viscoelastic free surface flows we simulate the extrudate swell of a planar jet emerging from a die.

We consider the time-dependent flow of a two-dimensional jet flowing through a slit and extruded into air. The no-slip condition is imposed on the wall of the slit while fully developed flow is imposed at the fluid entrance (see equations (43) and (44)). On the fluid free surface we imposed the full stress conditions (see Eqs. (16) and (17)). The flow domain is sketched in Fig. 6.

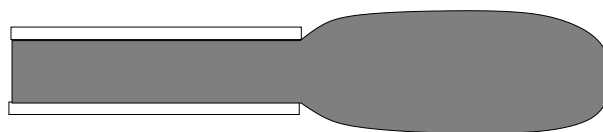


**Figure 6.** Definition of the flow domain for the extrudate swell simulation.

The following input data were employed: Slit width:  $L = 10$  mm;  $\delta x = \delta y = 1$  mm Poisson solver tolerance  $EPS = 10^{-7}$ ; Fluid definition:  $\mu_0 = 0.01$  Pas,  $\rho = 1$  Kgm $^{-3}$ ,  $\lambda_1 = 0.01$  s,  $\lambda_2 = 0.005$  s; scaling parameters:  $L = 0.01$  m,  $U = 1$  ms $^{-1}$ ,  $\mu_0 = 0.01$  Pas and gravity effects we neglected. Hence,  $Re = 1$  and  $We = 1$ . We observe that the value of  $We = 1$  used in this simulation is not the effective Weissenberg number. The effective Weissenberg number for the Oldroyd-B model, as pointed out by Yoo and Na (1991), is

$$We_{\text{effect}} = \left(1 - \frac{\lambda_2}{\lambda_1}\right) We.$$

Thus, in this simulation we used  $We_{\text{effect}} = 0.5$ . The results of this simulation are displayed in Fig. 7. Figure 7 shows different time frames of the jet flowing through the slit and then being extruded into the air. As the calculation proceeds the fluid jet undergoes large swelling deformation due to viscoelasticity; the final frame in Fig. 4 shows the jet at the later time  $t = 0.34$  s where the jet has achieved the maximum swelling ratio of  $S_r = D_{max}/L = 1.69$ .

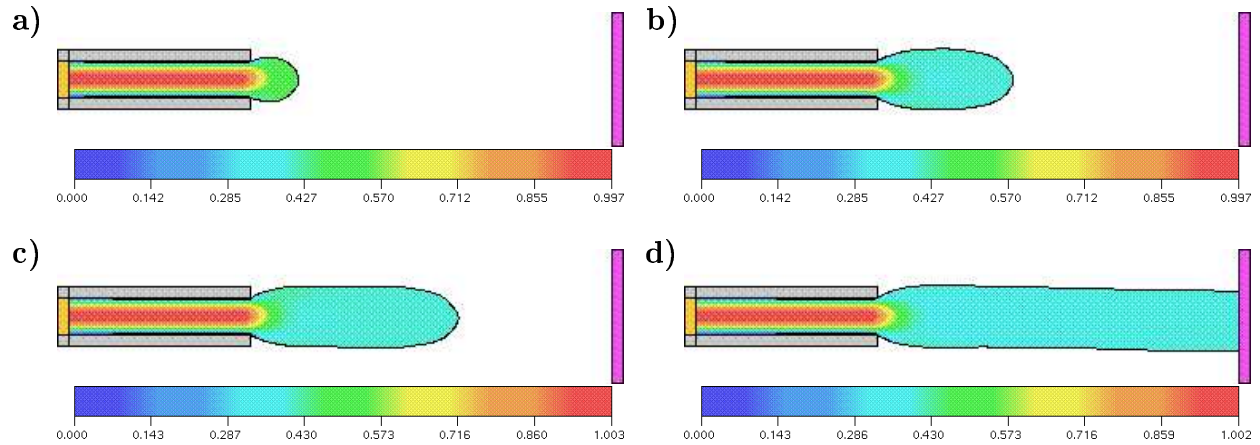


**Figure 4.** Numerical simulation of the channel flow. Fluid surface and velocity contours of the  $u$ -velocity at times: a)  $t = 0.09$  s, b)  $t = 0.15$  s, c)  $t = 0.20$  s and d)  $t = 0.34$  s.

## 7. Concluding Remarks

This paper has been concerned with the implementation of a numerical method for solving viscoelastic free surface flows into the FREEFLOW2D code. In particular, we have been dealing with flows governed by the Oldroyd-B model. The finite difference method described has improved the technique presented by Tomé et al. (2002) in several ways: we have replaced the explicit Euler solver by the explicit modified Euler method, obtaining a second order method for calculating the intermediate velocities; the same procedure was applied to compute the components of the non-Newtonian extra stress tensor. By using local Taylor series expansions, the derivatives  $\frac{\partial^2 v}{\partial y^2}$  and  $\frac{\partial^2 v}{\partial x^2}$  in Eqs. (18)-(19) are obtained by second order schemes; the same treatment has been used to compute the derivatives  $\frac{\partial u}{\partial y}$  and  $\frac{\partial v}{\partial x}$  when calculating the non-Newtonian stress on rigid boundaries. The implementation has been validated by simulating the flow of an Oldroyd-B fluid inside a channel and the numerical results were compared to the analytic values of a fully developed flow. We used  $We = 2$  and performed mesh refinement and the results demonstrated convergence of the numerical method. To demonstrate that the numerical method presented in this paper can simulate viscoelastic free surface flows we simulated the classical extrudate swell problem. We used  $We_{\text{effect}} = 0.5$  and a grid containing 10 points inside the slit and obtained a swelling ratio  $S_r = 1.69$ . Tomé et al. (2002) has simulated this same problem using a grid with 20 points inside the slit and obtained  $S_r = 1.69$ . Thus, the implementation described in this paper produced the same result using a coarser grid.

## References

- Amsden, A. and Harlow, F., 1970, "The SMAC Method: A Numerical Technique for Calculating Incompressible Fluid Flows", Los Alamos Scientific Laboratory Report La- 4370, Los Alamos, New Mexico.
- Asaithamb, N.S. 1987, "Computation of Free-Surface Flows", J. Comp. Phys., **73**, 380-394.
- Batchelor, G.K., 1967, "An Introduction to Fluid Dynamics", C.U.P., Cambridge.
- Brasseur, E., Fyrrillas, M.M., Georgiou, G.C. and Crochet, M.J., 1998, "The time-dependent extrudate-swell problem of an Oldroyd-B fluid with slip along the wall, J. Rheol., **42:3**, pp. 549-566.
- Castelo, A., Tomé, M.F., César, C.N.L., McKee, S. and Cuminato, J.A., 2000, "Freeflow: An integrated simulation system for three-dimensional free surface flows", Computing and Visualization in Science, **2**, pp. 199-210.
- Chan, R.K. and Street, R.L., 1971, "A Computer Study of Finite Amplitude Water Waves", J. Comp. Phys., **6**, pp. 68.
- Ferreira, V.G., Tomé, M.F., Mangiavacchi, N., Castelo, A., Cuminato, J.A., Fortuna, A. and McKee, S., "High Order Upwinding and the Hydraulic Jump", Intern. J. Numer. Meth. Fluids, vol. 39, pp. 549-583.
- Fritts, M.J. and Boris, J.P., 1979, "The Lagrangian Solution of Transient Problems in Hydrodynamics Using a Triangular Mesh", J. Comp. Phys., **31**, pp. 73-215.

- Harlow F. and Welch, J.E., 1965, "Numerical Calculation of time-dependent viscous incompressible flow of fluid with a free surface", *Phys. Fluids*, **8**, pp. 2182-2189.
- Hirt, C.W. and Nichols, B.D., 1981, "Volume of Fluid (VOF) Method for the Dynamics of Free Boundaries", *J. Comp. Phys.*, **39**, pp. 201.
- Kang, I.S. and Leal, L.G., 1987, "Numerical Simulation of Axisymmetric, Unsteady Free-Boundary Problem at Finite Reynolds Number. I. Finite-Difference Scheme and Its Application to the Deformation of a Bubble in a Uniaxial Straining Flow", *Phys. Fluids*, **30**, pp. 1929-1940.
- Miyata, H. and Nishimura, S. 1985, "Finite-Diference Simulation of Non-linear Waves Generated by Ships of Arbitrary Three-Dimensional Configuration", *J. Comp. Phys.*, **60**, pp. 391.
- Mompean, G. and M. Deville, M., 1997, "Unsteady finite volume of Oldroyd-B fluid through a three-dimensional planar contraction", *J. Non-Newtonian Fluid Mech.*, **72**, pp. 253-279.
- Oguz, H.N. and Prosperetti, A., 1993, "Dynamics of bubble growth and detachment from a needle", *J. Fluid Mech.* **257**, pp. 111-145.
- Tomé, M.F. and McKee, S., 1994, "GENSMAC: A computational marker-and-cell method for free surface flows in general domains", *J. Comput. Phys.*, **110**, pp. 171-186.
- Tomé, M.F., Duffy, B.R. and McKee, S., 1996, "A numerical technique for solving unsteady non-Newtonian free surface flows", *J. Non-Newtonian Fluid Mech.*, **62**, pp. 9-34.
- Viecelli, J.A., 1971, "A Method for Including Arbitrary External Boundaries in the MAC Incompressible Fluid Computing Technique", *J. Comp. Phys.*, **8**, pp. 119.
- Yoo, J.Y. and Na, Y., 1991, "A numerical study of the planar contraction flow of a viscoelastic fluid using the SIMPLER algorithm", *J. Non-Newtonian Fluid Mech.*, **30**, pp. 89-106.